Sustainable Energy & Fuels

ROYAL SOCIETY OF CHEMISTRY

PAPER

View Article Online
View Journal | View Issue

Check for updates

Cite this: *Sustainable Energy Fuels*, 2024, **8**, 1048

Low-grade waste heat recovery for wastewater treatment using clathrate hydrate based technology†

Lingjie Sun, [ab] Aliakbar Hassanpouryouzband, [*b] Tian Wang,[a] Fan Wang,[ac] Lunxiang Zhang,[*a] Chuanxiao Cheng,[d] Jiafei Zhao [a] and Yongchen Song[*a]

Effectively recycling low-grade waste heat is crucial for advancing decarbonization and achieving net-zero emissions, yet current methodologies are limited by inefficiencies in extracting energy from sources with low exergy. This study introduces an innovative approach leveraging hydrate formation and dissociation to utilize low-grade waste heat in purifying wastewater. By directly heating (low-grade waste heat) liquid R134a, our method induces bubble formation, thereby enhancing hydrate nucleation and growth. Our system demonstrates exceptional energy efficiencies, reaching up to 23.5%, and exhibits a high removal efficiency for wastewater with high concentrations of organic and heavy metal contaminants, including methylene blue (86.4%), Cr^{3+} (98.0%), Ni^{2+} (98.3%), Zn^{2+} (98.0%), and Cu^{2+} (97.1%). This approach not only offers a sustainable pathway for waste heat utilization but also addresses critical challenges in wastewater treatment. This technology demonstrates substantial potential in both low-grade waste heat recovery and wastewater treatment.

Received 6th November 2023
Accepted 22nd January 2024

DOI: 10.1039/d3se01440a

rsc.li/sustainable-energy

Introduction

Modern society grapples with significant energy and environmental challenges, largely arising from industrial growth. Industrial development, while driving the global economy, contributes substantially to primary energy consumption and CO_2 emissions.[1,2] Over 130 countries have adopted or are considering ambitious targets, such as net-zero emissions or climate neutrality, to mitigate climate change.[3,4] Approximately 50% of the energy input in industrial operations dissipates as waste heat, contributing to a significant energy waste.[1,5] Notably, low-temperature waste heat (<100 °C), comprising about 156 EJ (roughly 63% of total waste heat), remains largely untapped.[6] Therefore, improvements in energy efficiency and waste heat recovery are crucial for achieving net-zero emissions.[7]

Industrial waste heat is typically classified into high-grade (T > 673 K), medium-grade (373 K < T < 673 K), and low-grade (T < 373 K) categories.[8,9] Low-grade heat constitutes over 50% of the total dissipated heat resources.[10] Established technologies like heat pumps,[11] steam turbines,[12] and organic rankine cycles (ORCs)[13] can effectively harness high-grade and medium-grade waste heat due to their elevated temperatures. Conversely, low-grade waste heat recovery poses significant challenges owing to its proximity to ambient temperature.[8] While adsorption chillers for refrigeration have been employed to utilize low-grade waste heat above 333 K,[14–17] their adoption is limited by low efficiency and large physical footprint. Novel technologies such as thermoelectric materials,[8,18,19] chemical conversion approaches,[20] and thermally regenerative electrochemical cycles[21] have emerged as potential solutions for converting low-grade waste heat into power. In recent years, membrane distillation (MD), which uses low-grade heat energy for desalination or wastewater treatment as a sustainable alternative to fossil fuels, has gained increasing attention. This interest aligns with sustainable energy policies.[22,23] The MD method has demonstrated promising results, achieving water recovery rates of up to 92.8% in treating ion exchange regeneration effluent from power stations.[24] Despite these advancements, challenges such as membrane fouling and scaling, which can decrease flux and compromise water quality, persist.[24,25] While these technologies mark significant advancements in using low-grade waste heat for energy recovery, their energy efficiency and cost-effectiveness require further enhancement.[26,27] However, when compared to these emerging methods, traditional approaches

[a]*Key Laboratory of Ocean Energy Utilization and Energy Conservation of Ministry of Education, School of Energy and Power Engineering, Dalian University of Technology, Dalian 116024, China. E-mail: lunxiangzhang@dlut.edu.cn; songyc@dlut.edu.cn*

[b]*School of Geosciences, University of Edinburgh, Grant Institute, West Main Road, Edinburgh EH9 3FE, UK. E-mail: Hssnpr@ed.ac.uk*

[c]*School of Mechanical and Aerospace Engineering, Nanyang Technological University, 50 Nanyang Avenue, 639798, Singapore*

[d]*School of Energy and Power Engineering, Zhengzhou University of Light Industry, Zhengzhou, 450002, China*

† Electronic supplementary information (ESI) available. See DOI: https://doi.org/10.1039/d3se01440a

like organic rankine cycles (operating at 373 K–393 K) and thermally regenerative electrochemical cycles, though relatively mature, show markedly lower efficiency. These established systems are capable of converting only 2–9% of waste heat into power.[28] This disparity highlights the urgent need for innovative technologies that can achieve higher recovery efficiencies, improved economic performance, and enhanced practical feasibility. Clathrate hydrates are crystalline compounds with an ice-like solid structure formed by capturing guest molecules (such as CH_4, CO_2, and C_3H_8) within a cage-like framework of hydrogen-bonded water molecules, typically under conditions of high pressure or low temperature.[29,30] Pure hydrates consist solely of water and guest molecules, offering unique structural characteristics.[31] This characteristic has made hydrate-based desalination a promising method, where treated water is derived through hydrate formation, separation, and dissociation.[32,33] Previous studies have reported desalination removal efficiencies of over 80%, with freshwater recovery rates exceeding 30%.[34] Despite extensive research on hydrate-based methods for desalination, limited literature has focused on wastewater treatment. Our preliminary experiments in organic wastewater treatment using hydrates have achieved removal efficiencies above 90%,[35,36] yet the broader application of hydrates faces challenges due to slow formation rates. This sluggishness is largely ascribed to the random nature of crystal nucleation and constraints in heat and mass transfer. While strategies like the use of kinetic promoters or new guest molecules have shown promise in accelerating hydrate formation,[33] some approaches may not be feasible for water treatment. Despite these challenges, the distinctive attributes of hydrates have captured significant attention in fields such as desalination,[32] gas storage,[30] cold storage,[37] gas separation,[38] sludge dewatering[39] and CO_2 capture,[31] aligning with the goal of net-zero emissions.[31] Thus, overcoming the challenge of slow hydrate formation, a key obstacle stemming from unpredictable nucleation and heat and mass transfer inefficiencies, is essential for the practical deployment of hydrate-based technologies.

Crystal nucleation is an intricate stochastic process driven by density and energy fluctuations, involving the direct assembly of monomers across surface and volume free-energy barriers.[40] Under static conditions, the presence of nucleation barriers and critical nuclei presents formidable challenges for crystal formation. However, physical perturbations, such as stirring and shear flows, can promote nucleation and significantly reduce the induction time.[30–32] Crystal growth, an amalgamation of matter and energy transfer, is influenced by various factors. Boiling, renowned for its strong convective heat transfer properties, stands out as a formidable source of disturbance.[41] During the boiling process, the rapid formation of voluminous bubbles culminates in their ascent to the free surface, where they rupture, releasing their vapor content and yielding maximal heat flux. The dynamic interplay of bubble generation, movement, and collapse serves to augment mass and heat transfer processes.[42]

In this study, we present a groundbreaking approach for harnessing extra low-grade waste heat below 343 K to facilitate the production of clean water from industrial wastewater, leveraging the power of hydrate technology. The utilization of extra low-grade waste heat induces the ebullition of liquid guest molecules, thereby promoting hydrate nucleation and formation through enhanced mass and heat transfer phenomena.

The mechanism of enhanced hydrate formation, the system energy efficiency, and the removal efficiency for high concentrations of wastewater were analyzed. These remarkable findings underscore the immense potential of this innovative technology in various domains, including low-grade waste heat recovery, low-temperature CO_2 capture, seawater desalination, and sewage treatment.

Materials and methods

Materials and apparatus

The simulated wastewater was prepared by adding a certain amount of methylene blue, Hexahydrate chromium trichloride ($CrCl_3 \cdot 6H_2O$, 99.0%), nickel sulfate hexahydrate ($NiSO_4 \cdot 6H_2O$, 98.5%), zinc sulfate heptahydrate ($ZnSO \cdot 7H_2O$, 99.5%), and copper sulfate pentahydrate ($CuSO_4 \cdot 5H_2O$, 99.0%) to deionized water. More detailed information can be found in the ESI.† Deionized water (dw) was sourced from an in-lab water purification system (Aquapro2S, Aquapro International Company LLC, USA). Hydrate formation was facilitated within a high-pressure chamber possessing an internal volume of 7710 mL. The source of waste heat was substituted with a consistent heat source provided by a pair of 200 W-rated electric heaters, designed to accurately simulate diverse temperature heat resources. Chamber temperature control was enabled through a water bath (XT5718RCE800L, Xutemp, Hangzhou, Co., Ltd). The course of the experiment was diligently documented using a digital camera (EOS 6D, Canon Company, lens model EF24-105 mm f/4L IS USM, Japan). Additional detailed information is available in the ESI.†

Experimental setup and procedures

Fig. 1 illustrates that our system comprises two primary components: a wastewater treatment system for producing clean water, and a heat system for harnessing low-grade waste heat and facilitating hydrate formation. R134a, recognized for its superior boiling and condensation properties and extensive use in refrigeration,[43] serves as the guest molecule in our study. It was chosen for hydrate formation in wastewater due to its favorable formation conditions and cost-effectiveness.[35,36] The process converts water molecules into solid hydrate with R134a molecules. Notably, pure hydrates consist solely of water and guest molecules,[29–31] which enables the production of clean water following separation and hydrate dissociation. The treated water and R134a can be collected and reused, promoting a closed-loop system. For more in-depth details on hydrate-based wastewater treatment, refer to our previous publications and the provided ESI.†[35]

The second component of our system is the heating mechanism located at the bottom of the chamber, as depicted in Fig. 1b. The passage of hot water or steam through the base heats the underlying surface. This heat is then conducted to the liquid R134a in contact with this surface, triggering its boiling. Due to the buoyancy effect, bubbles ascend through the liquid

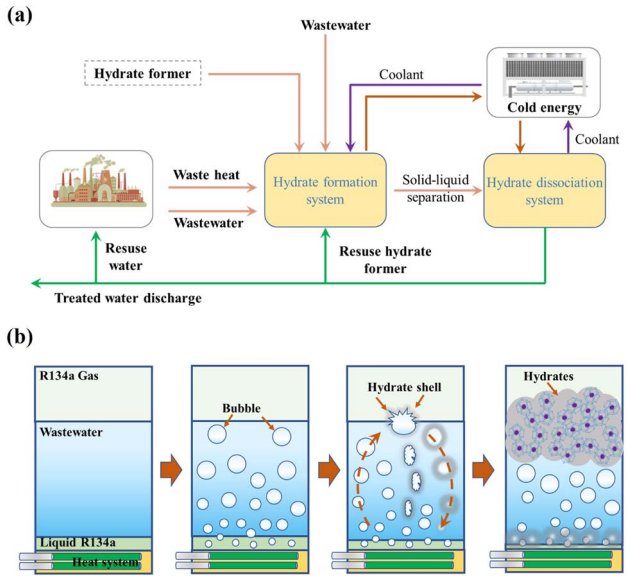

Fig. 1 (a) Industrial flowsheet using hydrate-based technology for low-grade waste heat recovery and water reclamation from wastewater. Stepwise wastewater treatment procedure: hydrate formation, solid–liquid separation, hydrate dissociation; (b) schematic diagram illustrating hydrate formation *via* low-grade waste heat: the waste heat is directly applied to heat the liquid hydrate former, triggering bubble generation. The energy disturbance, resultant from bubble collapse, can facilitate crystal embryos to overcome the crystal-nucleation barrier and the critical nucleus barrier, thereby accelerating hydrate formation.

region. During this ascent, they encounter colder liquid layers, resulting in a gradual decrease in volume, sometimes to the point of rupture. Simultaneously, hydrate shells rapidly encapsulate these bubbles. These shells possess a fragile and porous structure, composed of overlapping flakes of gas hydrate.

A volume of 4000 mL of simulated wastewater was introduced into the chamber, followed by the injection of R134a gas at 0.5 MPa and a temperature of 275 K. Subsequently, the electric heaters were engaged to elevate the temperature of the liquid R134a until the bottom layer approached 281 K. At this point, the electric heaters were deactivated. Following the formation of the hydrate, a liquid–solid separation procedure was employed to isolate pure hydrate. The final step involved the dissociation of pure hydrate into water and R134a.

Measurements and analysis

The absorption spectra of methylene blue in the wastewater were documented employing a UV-Vis-NIR spectrophotometer (Lambda750S, USA). The concentrations of various heavy metals present in the wastewater were quantified using an inductively coupled plasma optical spectrometer (ICP, AVIO 500, PerkinElmer, USA).

Calculations

Comprehensive insights into the efficiency of wastewater treatment and energy utilization can be found as follows.

The thermal energy required for heating wastewater and R134a is calculated using eqn (1) and (2):

$$Q_w = \int_{T_1}^{T_2} m_w C_w dT \quad (1)$$

$$Q_R = \int_{T_1}^{T_2} m_{R134a} C_{R134a} dT \quad (2)$$

where Q_w and Q_R represent the energy absorbed for heating wastewater and R134a, respectively. C_w and C_{R134a} denote the specific heat capacities of wastewater and R134a, while m_w and m_{R134a} are their masses. T_1 and T_2 indicate the initial and final temperatures after heating cessation. The energy consumption for hydrate formation is then derived using eqn (3) and (4):

$$Q_{absorb} = Q_w + Q_R + Q_{R134a} \quad (3)$$

$$Q_{resource} = \int_{t_1}^{t_2} q dt \quad (4)$$

In these equations, Q_{absorb} is the total absorbed energy and Q_{R134a} represents the latent heat of vaporization of R134a. The integral $\int_{t_1}^{t_2} q dt$ accounts for the total heat supplied by the heat source from time t_1 to t_2. It is assumed that the conversion rate of hydrate is 80%.[44,45]

Thus, the thermodynamic energy efficiency of low-grade waste heat harvesting could be expressed as:

$$\eta_E = \frac{Q_{absorb}}{Q_{resource}} \quad (5)$$

Results and discussion

Boiling heat transfer stands out as a potent mechanism for extracting substantial thermal energy from a surface, primarily due to its high heat transfer coefficient. A significant quantity of thermal energy is transferred directly to the liquid water through thermal convection induced by bubble boiling.[41,42] Previous research has established that bubble formation plays a critical role in enhancing the nucleation and growth of gas hydrates.[46,47] In this study, the low-grade waste heat was used to generate gas bubbles to promote hydrate formation, as shown in Fig. 2. Three thermocouples were inserted at different locations in the chamber to monitor the temperature trajectories. A pressure transducer was attached to the top of the chamber to monitor the pressure changes during hydrate formation.

Fig. 2a shows the temperature and pressure conditions during the experimental procedure. During gas injection from the top of the chamber, the temperature at the top and middle positions increased due to the Joule-Thomson effect. The temperature at the bottom position remained steady. With the pressure increase during gas injection, gaseous R134a gradually liquefied and accumulated at the bottom of the reactor due to the density difference between liquid water and R134a, as shown in Fig. 2b. After gas injection, the temperature at the top and middle positions decreased. Upon the initiation of heating,

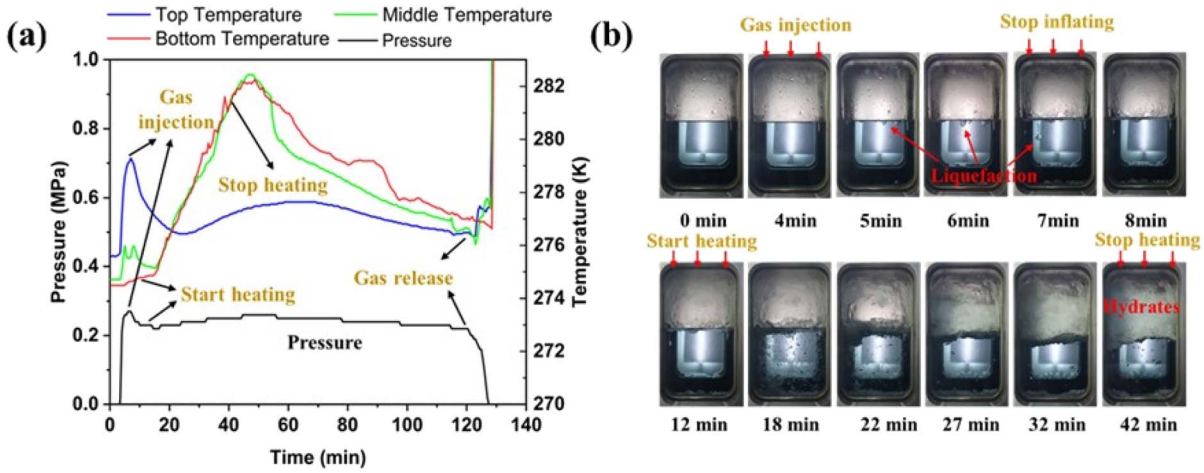

Fig. 2 Enhanced hydrate formation utilizing low-grade waste heat. (a) Graph depicting the temperature and pressure trends throughout the hydrate formation process. (b) Sequential photographic representation showing bubble dynamics and the morphology of hydrate formation. Post-heating, a profusion of bubbles forms, rises, and bursts within the fluid.

the temperature at the chamber's bottom rose from 274.8 K to 281.7 K. As the temperature rose, a large amount of liquid R134a vaporized and began to produce bubbles, as shown in Fig. 2b. This period coincided with the formation of numerous bubbles. These bubbles ascended swiftly, bursting upon reaching the liquid–gas interface, and were promptly succeeded by hydrate formation. The temperature in the middle position of the chamber also increased to nearly 282 K due to the boiling heat transfer. Massive amounts of hydrates formed during the heating period. Notably, R134a begins to dissociate if the temperature exceeds 283 K at 0.38 MPa (absolute pressure).[35] Therefore, the maximum temperature was maintained below 283 K. Subsequently, the heating stopped, resulting in a decrease in temperature at the bottom and middle. Finally, the bubbles produced by boiling heat transfer and the hydrate formation rate also decreased.

The hydrate formation rate is limited by mechanisms of intrinsic kinetics and mass and heat transfer. For hydrophobic gas guest molecules with relatively low solubility in water, a sufficient concentration in water is required to form hydrates. During hydrate formation, the gas concentration in water can be hundreds of times its solubility. Previous literature proved that the presence of bubbles in hydrate-dissociated water can provide massive amounts of gas molecules for hydrate formation.[46,47] On the other hand, it is difficult for hydrate nucleation to occur in a static state. Under gas-saturated or water-saturated conditions, the formed hydrate will cover the gas–water interface, hindering mass transfer and further hydrate formation, as shown in Fig. 3a and b. Thus, some methods such as mechanical stirring, bubbling, or pressure oscillation can promote hydrate nucleation and reduce induction time.

In this study, low-grade waste heat was used to generate gas bubbles to promote hydrate formation. Continuous bubbles were generated by boiling from the bottom of the chamber. The bubbles would break up once they rose to the gas–liquid interface at the top of the cell. The breakage frequency of

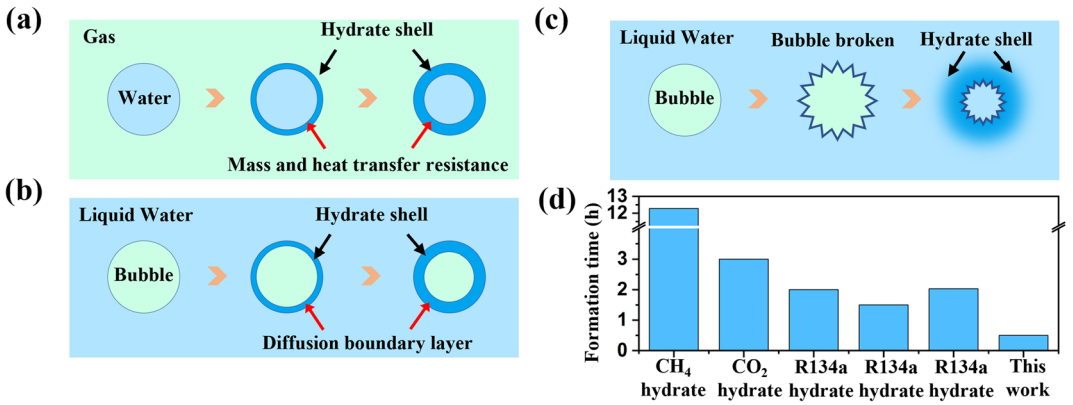

Fig. 3 The schematic diagram of hydrate formation under different conditions; (a–c) Schematic diagrams representing the mass and heat transfer barriers under varying formation conditions; the development of a hydrate shell in conditions (a) and (b) inhibits heat and mass transfer, while bubble rupture in condition (c) overcomes mass transfer resistances, augmenting the diffusion contact area. (d) A comparative analysis of formation times across different hydrate formers and methods.

bubbles at the gas/liquid interface increased with the heat flux, increasing the turbulence in the chamber. Bubble rupture, akin to an explosion, released vast amounts of energy and substances into the liquid water. The energy disturbance caused by this bubble collapse helped crystal embryos surpass the crystal-nucleation and critical nucleus barrier,[48–50] thereby reducing the induction time for hydrate crystals. In addition, bubble rupture disseminated more R134a molecules into the water, enhancing the contact area between R134a and water molecules. This increased mass and heat transfer rate expedited hydrate formation, enabling this method to surmount the mass and heat transfer barrier, as depicted in Fig. 3c–e. As a result, the hydrate formation time was slashed to 30 minutes, just a quarter of the time taken by traditional methods.[51–55]

Subsequent to hydrate formation, a variety of separation methods were employed to isolate the solid hydrate from the liquid. Clean water was obtained through hydrate dissociation. Fig. 4 shows the removal efficiency achieved through different separation methods. The maximum removal efficiency exceeded 90% for heavy metal wastewater. For organic or mixed organic-heavy metal wastewaters, the removal efficiency was analogous, demonstrating the extensive applicability of the hydrate method for diverse wastewater types. The dissociated water could be reclaimed and reused. After several cycles of hydrate formation and decomposition, it was even possible to obtain pure water. For more detailed information on wastewater treatment based on hydrates, please refer to our previous work.[35]

Energy utilization efficiency represents a pivotal metric in assessing low-grade waste heat utilization technologies. Despite persistent advancements, energy efficiency remains constrained due to thermodynamic limitations, primarily arising when the heat source's temperature approximates ambient conditions.[3,5] Conventional methodologies result in a substantial loss of exergy.[6] In this study, we introduce an equation (eqn (6)) to evaluate the thermodynamic energy efficiency of low-grade waste heat harvesting, founded on the hydrate-based method. A more comprehensive breakdown of the calculation procedure can be found in the ESI.†

$$\eta_E = \frac{Q_{absorb}}{Q_{resource}} = \frac{\int_{T_1}^{T_2} C_{R134a}\mathrm{d}T + \int_{T_1}^{T_2} C_w\mathrm{d}T + Q_{R134a}}{\int_{t_1}^{t_2} q\mathrm{d}t} \quad (6)$$

where $\int_{T_1}^{T_2} C_{R134a}\mathrm{d}T$ and $\int_{T_1}^{T_2} C_w\mathrm{d}T$ are the sensible heat of R134a and water liquid absorbed by the temperature rise from temperature T_1 to T_2. Q_{R134a} is the latent heat of vaporization of R134a. $\int_{t_1}^{t_2} q\mathrm{d}t$ is the total heat provided by the heat source from time t_1 to t_2.

For a comprehensive comparison of our approach with alternative methods, we present the total energy efficiency in Fig. 5. The organic rankine cycle (ORC), a traditional thermal-electricity conversion method, has been widely used for half a century. It utilizes low-grade heat to heat low-boiling-point organic working fluids to produce steam, subsequently generating electricity in a turbine. Due to condensing temperature and pressure requirements, typically less than 10% of the heat is converted to electricity. The conventional ORC system demonstrates maturity and superior performance compared to other methods when waste heat temperatures exceed 573 K. However, approximately 90% of low-grade waste heat exists below 573 K.[56] This is uneconomical for waste-heat recovery using the traditional Rankine cycle. Hence, researchers are still exploring other alternative technologies.

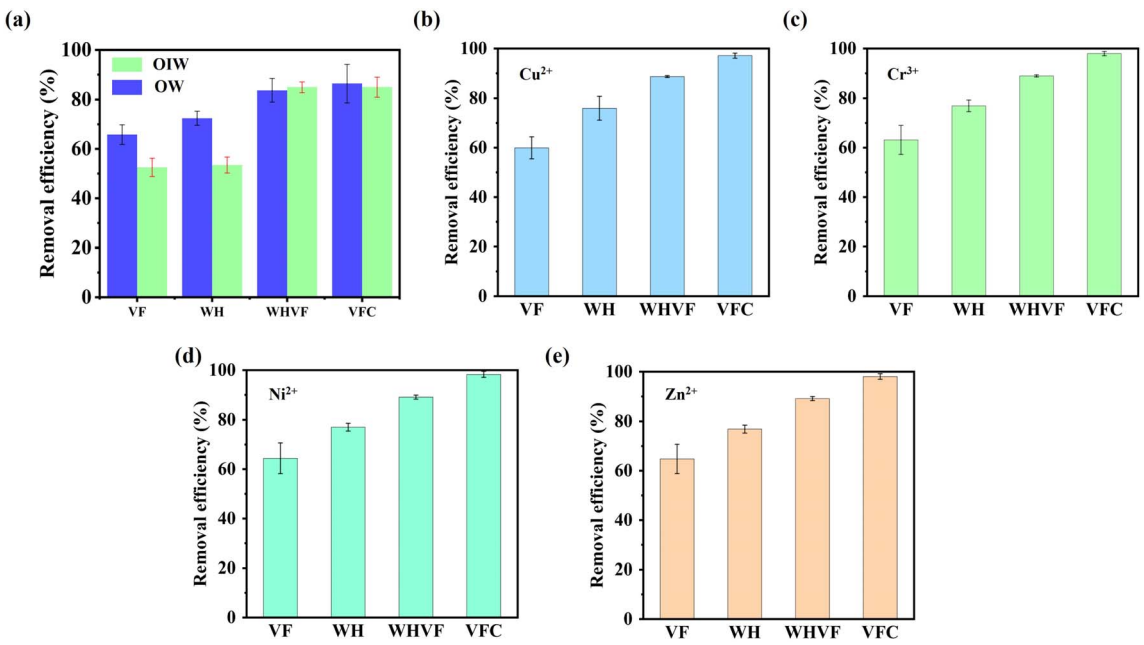

Fig. 4 Efficiency of pollutant removal across varying wastewater types: (a) efficiency in the removal of methylene blue from simulated organic wastewater (OW) and organic–inorganic wastewater (OIW); (b–e) efficiency in the removal of Cu^{2+}, Cr^{3+}, Ni^{2+}, and Zn^{2+} from simulated organic–inorganic wastewater.

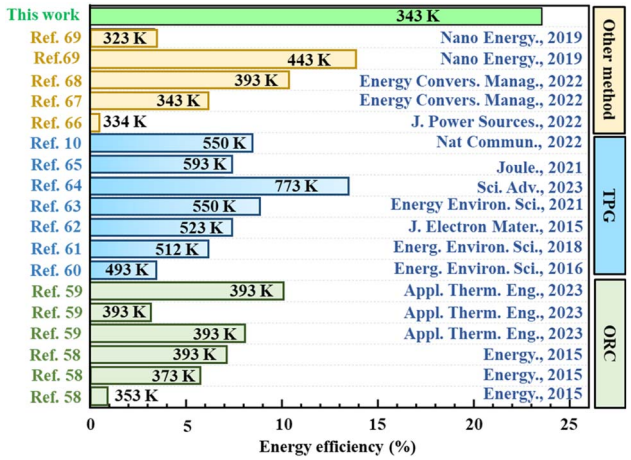

Fig. 5 Comparison of the energy efficiency of this study and literature results.

In recent years, as a clean and silent energy conversion technology, thermoelectric materials have shown the capability to directly convert heat into electricity, making them attractive for recycling low-grade waste heat and power generation. Thermoelectric energy conversion exploits the Seebeck effect to convert thermal energy into electricity. While many thermoelectric materials have been developed, they are primarily at a laboratory level. Other emerging methods, such as carbon capture with a waste heat utilization system, thermally regenerative ammonia batteries, or reverse electrodialysis heat engines, are also dedicated to industrial waste heat utilization fields. Unfortunately, the energy recovery efficiencies of these methods remain below 10% when operating below 373 K.[57]

In this study, low-grade waste heat was employed to directly heat liquid R134a until it reached its boiling point. The low boiling point of R134a allows utilization of low-grade waste heat even below 373 K. Moreover, the boiling process constitutes a direct heat-exchange process, thereby minimizing heat transfer losses. At a hot-side temperature of 373 K, the energy efficiency reaches 23.5%, surpassing the efficiencies achieved by other methods.[10,58–69] If the share of the actual projected angle of the total heat flow from the heating rod to the bottom of the reactor is considered, the theoretical energy efficiency should be 51.4%. By directly heating R134a using low-grade waste heat, without the need for an intermediate circuit, this method sidesteps the heat transfer constraints associated with ambient temperature and minimizes heat loss. Moreover, the approach does not necessitate intricate equipment. Given the affordability of R134a, this method holds significant commercial potential for harnessing low-grade heat energy, whilst concurrently facilitating the production of clean water from industrial wastewater.

Conclusions

In this study, we have presented innovative strategies for harnessing low-grade waste heat through a hydrate-based method. This approach allows the direct use of low-grade waste heat to form hydrates in heavy metal–organic wastewater, with clean water subsequently obtained through hydrate dissociation. Notably, system energy efficiencies can reach up to 23.5%. The treatment of each ton of wastewater absorbs 42 365 kJ of waste heat, equivalent to reducing carbon dioxide emissions by 39 031 tons. Importantly, full implementation of this method can be accomplished using existing equipment, eliminating the need for new complex machinery or advanced materials. Through this work, we highlight the immense potential of the hydrate-based method in waste heat recovery applications, all the while effectively addressing wastewater treatment.

Author contributions

L. J. Sun performed the experiments and wrote the manuscript. Dr A. Hassanpouryouzband helped revised the manuscript. T. Wang, F. Wang and Chuanxiao Chen assisted with the experiments. A. Hassanpouryouzband and L. X. Zhang helped revise the manuscript. J. F. Zhao and Y. C. Song planned, supervised, and led the project.

Conflicts of interest

The authors declare no competing financial interest.

Acknowledgements

This study was supported by the National Natural Science Foundation of China (grant no. 52025066, 52020105007, 52006024). Lingjie Sun acknowledges the support of the state scholarship fund from the China Scholarship Council (no. 202206060072). This project received partial support from UKCCS through the CRYSTAL-CCS project funding.

References

1 Z. Xu, R. Wang and C. Yang, Perspectives for low-temperature waste heat recovery, *Energy*, 2019, **176**, 1037–1043.
2 M. Wise, K. Calvin, A. Thomson, L. Clarke, B. Bond-Lamberty, R. Sands, S. Smith, A. Janetos and J. Edmonds, Implications of Limiting CO_2 Concentrations for Land Use and Energy, *Science*, 2009, **324**, 1183–1186.
3 J. Rosenow and N. Eyre, Reinventing energy efficiency for net zero, *Energy Res. Soc. Sci.*, 2022, **90**, 102602.
4 H. Van Soest, M. den Elzen and D. van Vuuren, Net-zero emission targets for major emitting countries consistent with the Paris Agreement, *Nat. Commun.*, 2021, **12**, 2140.
5 M. Imran, M. Usman, B. Park and D. Lee, Volumetric expanders for low grade heat and waste heat recovery applications, *Renewable Sustainable Energy Rev.*, 2016, **57**, 1090–1109.
6 C. Geffroy, D. Lilley, P. Parez and R. Prasher, Techno-economic analysis of waste-heat conversion, *Joule*, 2021, **12**, 3080–3096.
7 M. Albert, K. Bennett, C. Adams and J. Gluyas, Waste heat mapping: A UK study, *Energy Res. Soc. Sci.*, 2022, **160**, 112230.

8 K. Mistewicz, M. Jesionek, M. Nowak and M. Kozioł, SbSeI pyroelectric nanogenerator for a low temperature waste heat recovery, *Nano Energy*, 2019, **64**, 103906.
9 R. Muhumuza and P. Eames, Decarbonisation of heat: Analysis of the potential of low temperature waste heat in UK industries, *J. Cleaner Prod.*, 2022, **372**, 133759.
10 Z. Bu, X. Zhang, Y. Hu, Z. Chen, S. Lin, W. Li, C. Xiao and Y. Pei, A record thermoelectric efficiency in tellurium-free modules for low-grade waste heat recovery, *Nat. Commun.*, 2022, **13**, 237.
11 Z. Tan, X. Feng and Y. Wang, Performance comparison of different heat pumps in low-temperature waste heat recovery, *Renewable Sustainable Energy Rev.*, 2021, **152**, 111634.
12 C. Laux, A. Gotter, F. Eckert and M. Neef, Experimental results of a low-pressure steam Rankine cycle with a novel water lubricated radial inflow turbine for the waste heat utilization of internal combustion engines, *Energy Convers. Manag.*, 2022, **271**, 116265.
13 C. Chen, P. Li and S. Le, Organic Rankine Cycle for Waste Heat Recovery in a Refinery, *Ind. Eng. Chem. Res.*, 2016, **55**(12), 3262–3275.
14 Q. Pan, J. Peng and R. Wang, Experimental study of an adsorption chiller for extra low temperature waste heat utilization, *Appl. Therm. Eng.*, 2019, **163**, 114341.
15 S. Yang, Y. Wang, J. Gao, Z. Zhang, Z. Liu and A. Olabi, Performance Analysis of a Novel Cascade Absorption Refrigeration for Low-Grade Waste Heat Recovery, *ACS Sustainable Chem. Eng.*, 2018, **6**(7), 8350–8363.
16 M. Arshad, M. Zaman, M. Rizwan and A. Elkamel, Economic optimization of parallel and series configurations of the double effect absorption refrigeration system, *Energy Convers. Manag.*, 2020, **210**, 112661.
17 E. Novek, E. Shaulsky, Z. Fishman, L. Pfefferle and M. Elimelech, Low-Temperature Carbon Capture Using Aqueous Ammonia and Organic Solvents, *Environ. Sci. Technol. Lett.*, 2016, **3**(8), 291–296.
18 Y. Zhou, X. Liu, B. Jia, T. Ding, D. Mao, T. Wang, G. Ho and J. He, Physics-guided co-designing flexible thermoelectrics with techno-economic sustainability for low-grade heat harvesting, *Sci. Adv.*, 2023, **9**, eadf5701.
19 F. Hao, P. Qiu, Y. Tang, S. Bai, T. Xing, H. Chu, Q. Zhang, P. Lu, T. Zhang, D. Ren, J. Chen, X. Shi and L. Chen, High efficiency Bi2Te3-based materials and devices for thermoelectric power generation between 100 and 300 °C, *Energy Environ. Sci.*, 2016, **9**, 3120–3127.
20 V. Haribal, X. Wang, R. Dudek, C. Paulus, B. Turk, R. Gupta and F. Li, Modified Ceria for "Low-Temperature" CO_2 Utilization: A Chemical Looping Route to Exploit Industrial Waste Heat, *Adv. Energy Mater.*, 2019, **9**, 1901963.
21 C. Gao, S. Lee and Y. Yang, Thermally Regenerative Electrochemical Cycle for Low-Grade Heat Harvesting, *ACS Energy Lett.*, 2017, **2**(10), 2326–2334.
22 A. Yadav, P. K. Labhasetwar and V. K. Shahi, Membrane distillation using low-grade energy for desalination: A review, *J. Environ. Chem. Eng.*, 2021, **9**(5), 105818.
23 D. U. Lawal and N. A. A. Qasem, Humidification-dehumidification desalination systems driven by thermal-based renewable and low-grade energy sources: A critical review, *Renewable Sustainable Energy Rev.*, 2020, **125**, 109817.
24 D. Noel, *et al.*, Pilot trial of membrane distillation driven by low grade waste heat: Membrane fouling and energy assessment, *Desalination*, 2016, **391**, 30–42.
25 K. Zhu, *et al.*, Low-Grade Waste Heat Enables Over 80 L m^{-2} h^{-1} Interfacial Steam Generation Based on 3D Superhydrophilic Foam, *Adv. Sci.*, 2023, **35**(29), 2211932.
26 A. Straub, N. Yip, S. Lin, J. Lee and M. Elimelech, Harvesting low-grade heat energy using thermo-osmotic vapour transport through nanoporous membranes, *Nat. Energy*, 2016, **1**, 16090.
27 Y. Liu, M. Cui, W. Ling, L. Cheng, H. Lei, W. Li and Y. Huang, Thermo-electrochemical cells for heat to electricity conversion: from mechanisms, materials, strategies to applications, *Energy Environ. Sci.*, 2022, **15**, 3670–3687.
28 J. Bleeker, S. Reichert, J. Veerman and D. Vermaas, Thermo-electrochemical redox flow cycle for continuous conversion of low-grade waste heat to power, *Sci. Rep.*, 2022, **12**, 7993.
29 E. D. Sloan, Fundamental principles and applications of natural gas hydrates, *Nature*, 2003, **426**, 353–359.
30 L. Sun, H. Sun, C. Yuan, L. Zhang, L. Yang, Z. Ling, J. Zhao and Y. Song, Enhanced clathrate hydrate formation at ambient temperatures (287.2 K) and near atmospheric pressure (0.1 MPa): Application to solidified natural gas technology, *Chem. Eng. J.*, 2022, 140325.
31 A. Hassanpouryouzband, E. Joonaki, M. V. Farahani, S. Takeya, C. Ruppel, J. H. Yang, N. J. English, J. M. Schicks, K. Edlmann, H. Mehrabian, Z. M. Aman and B. Tohidia, Gas hydrates in sustainable chemistry, *Chem. Soc. Rev.*, 2020, **49**, 5225–5309.
32 L. Sun, H. Sun, T. Wang, H. Dong, L. Zhang, L. Yang, J. Zhao and Y. Song, Self-Driven and Directional Transport of Water During Hydrate Formation: Potential Application in Seawater Desalination and Dewatering, *Desalination*, 2023, **548**, 116299.
33 S. M. Montazeri and G. Kolliopoulos, Hydrate based desalination for sustainable water treatment: A review, *Desalination*, 2023, **537**, 115855.
34 J. Zheng and M. Yang, Experimental investigation on novel desalination system via gas hydrate, *Desalination*, 2020, **478**, 114284.
35 L. Sun, H. Dong, Y. Lu, L. Zhang, L. Yang, J. Zhao and Y. Song, A hydrate-based zero liquid discharge method for high-concentration organic wastewater: resource recovery and water reclamation, *npj Clean Water*, 2023, **6**, 49.
36 H. Dong, L. Zhang, Z. Ling, J. Zhao and Y. Song, The Controlling Factors and Ion Exclusion Mechanism of Hydrate-Based Pollutant Removal, *ACS Sustainable Chem. Eng.*, 2019, **7**(8), 7932–7940.
37 C. Cheng, F. Wang, Y. Tian, X. Wu, J. Zheng, J. Zhang, L. Li, P. Yang and J. Zhao, Review and prospects of hydrate cold storage technology, *Renewable Sustainable Energy Rev.*, 2020, **117**, 109492.

38 A. Hassanpouryouzband, J. Yang, B. Tohidi, E. Chuvilin, V. Istomin, B. Bukhanov and A. Cheremisin, Insights into CO2 Capture by Flue Gas Hydrate Formation: Gas Composition Evolution in Systems Containing Gas Hydrates and Gas Mixtures at Stable Pressures, *ACS Sustainable Chem. Eng.*, 2018, **6**(5), 5732–5736.

39 L. Sun, A. Hassanpouryouzband, *et al.*, Advancement in Sewage Sludge Dewatering with Hydrate Crystal Phase Change: Unveiling the Micro-Moisture Migration and Dewaterability Mechanisms, *ACS Sustainable Chem. Eng.*, 2023, **11**(32), 12075–12083.

40 J. Sungho, T. Heo, *et al.*, Reversible disorder-order transitions in atomic crystal nucleation, *Science*, 2021, **371**, 498–503.

41 N. Quang, Q. Pham, S. Zhang, S. Hao, K. Montazeri, C. Lin, J. Lee, A. Mohraz and Y. Won, Boiling Heat Transfer with a Well-Ordered Microporous Architecture, *ACS Appl. Mater. Interfaces*, 2020, **12**(16), 19174–19183.

42 Q. Wang and R. Chen, Ultrahigh Flux Thin Film Boiling Heat Transfer Through Nanoporous Membranes, *Nano Lett.*, 2018, **18**(5), 3096–3103.

43 F. Pardo, G. Zarca and A. Urtiaga, Separation of Refrigerant Gas Mixtures Containing R32, R134a, and R1234yf through Poly(ether-block-amide) Membranes, *ACS Sustainable Chem. Eng.*, 2020, **8**(6), 2548–2556.

44 K. Jeong, Y. S. Choo, H. J. Hong, Y. S. Yoon and M. H. Song, Tetrafluoroethane (R134a) hydrate formation within variable volume reactor accompanied by evaporation and condensation, *Rev. Sci. Instrum.*, 2015, **86**, 035102.

45 F. Wang, X. Xia, Y. Lv, C. Cheng, L. Yang, L. Zhang, J. Zhao and Y. Song, Experimental study on the thermodynamic performance of a novel tetrabutylammonium bromide hydrate cold storage system, *J. Energy Storage*, 2022, 103980.

46 Y. Kuang, Y. Feng, L. Yang, Y. Song and J. Zhao, Effects of micro-bubbles on the nucleation and morphology of gas hydrate crystals, *Phys. Chem. Chem. Phys.*, 2019, **21**, 23401–23407.

47 W. Fu, Z. Wang, B. Sun and L. Chen, A mass transfer model for hydrate formation in bubbly flow considering bubble-bubble interactions and bubble-hydrate particle interactions, *Int. J. Heat Mass Transfer*, 2018, **127**, 611–621.

48 D. Lee, Y. Lee, S. Lee and Y. Seo, Accurate measurement of phase equilibria and dissociation enthalpies of HFC-134a hydrates in the presence of NaCl for potential application in desalination, *Korean J. Chem. Eng.*, 2016, **33**, 1425–1430.

49 G. C. Sosso, Ji Chen, S. J. Cox, M. Fitzner, P. Pedevilla, A. Zen and A. Michaelides, Crystal Nucleation in Liquids: Open Questions and Future Challenges in Molecular Dynamics Simulations, *Chem. Rev.*, 2016, **116**(12), 7078–7116.

50 C. Li, Z. Liu, E. Goonetilleke, *et al.*, Temperature-dependent kinetic pathways of heterogeneous ice nucleation competing between classical and non-classical nucleation, *Nat. Commun.*, 2021, **12**, 4954.

51 H. Roosta, S. Khosharay and F. Varaminian, Experimental study of methane hydrate formation kinetics with or without additives and modeling based on chemical affinity, *Energy Convers. Manag.*, 2013, **76**, 499–505.

52 P. Babu, R. Kumar and P. Linga, A New Porous Material to Enhance the Kinetics of Clathrate Process: Application to Precombustion Carbon Dioxide Capture, *Environ. Sci. Technol.*, 2013, **47**(22), 13191–13198.

53 J. Mok, W. Choi and Y. Seo, Theoretically achievable efficiency of hydrate-based desalination and its significance for evaluating kinetic desalination performance of gaseous hydrate formers, *Desalination*, 2022, **524**, 115487.

54 J. Li, D. Liang, K. Guo, R. Wang and S. Fan, Formation and dissociation of HFC134a gas hydrate in nano-copper suspension, *Energy Convers. Manag.*, 2006, **47**, 201–210.

55 S. Zafar, I. Dincer, and M. Gadalla, Crystal Growth Analysis of R134a Clathrate with Additives for Cooling Applications, in ed. F. Aloui and I. Dincer, *Exergy for A Better Environment and Improved Sustainability 2. Green Energy and Technology*, Springer, Cham, 2018.

56 S. Yang, S. Yang, Y. Wang and Y. Qian, Low grade waste heat recovery with a novel cascade absorption heat transformer, *Energy*, 2017, **130**, 461–472.

57 D. Huo, H. Tian, G. Shu and W. Wang, Progress and prospects for low-grade heat recovery electrochemical technologies, *Sustain. Energy Technol. Assessments*, 2022, **49**, 101802.

58 M. Yari, A. Mehr, V. Zare, S. Mahmoudi and M. Rosen, Exergoeconomic comparison of TLC (trilateral Rankine cycle), ORC (organic Rankine cycle) and Kalina cycle using a low grade heat source, *Energy*, 2015, **83**, 712–722.

59 J. Liu, Y. Zhang, H. Li, Y. Shuai, B. Li and T. Hung, Low-grade thermal energy utilization through using organic Rankine cycle system and R1233zd(E) at different heat source temperatures, *Appl. Therm. Eng.*, 2023, **230**, 120706.

60 F. Hao, *et al.*, High efficiency Bi2Te3-based materials and devices for thermoelectric power generation between 100 and 300 °C, *Energy Environ. Sci.*, 2016, **9**, 3120–3127.

61 R. Deng, *et al.*, High thermoelectric performance in Bi0.46Sb1.54Te3 nanostructured with ZnTe, *Energy Environ. Sci.*, 2018, **11**, 1520–1535.

62 X. Hu, *et al.*, Power Generation Evaluated on a Bismuth Telluride Unicouple Module, *J. Electron. Mater.*, 2015, **44**, 1785–1790.

63 Z. Bu, X. Zhang, Y. Hu, Z. Chen, S. Lin, W. Li and Y. Pei, An over 10% module efficiency obtained using non-Bi2Te3 thermoelectric materials for recovering heat of <600 K, *Energy Environ. Sci.*, 2021, **14**, 6506–6513.

64 C. Liu, *et al.*, Charge transfer engineering to achieve extraordinary power generation in GeTe-based thermoelectric materials, *Sci. Adv.*, 2023, **9**, eadh0713.

65 Z. Liu, *et al.*, Demonstration of ultrahigh thermoelectric efficiency of ~7.3% in Mg3Sb2/MgAgSb module for low-temperature energy harvesting, *Joule*, 2021, **5**, 1196–1208.

66 M. Rahimi, T. Kim, C. Gorski and B. Logan, A thermally regenerative ammonia battery with carbon-silver electrodes for converting low-grade waste heat to electricity, *J. Power Sources*, 2018, **373**, 95–102.

67 Z. Liu, D. Lu, Y. Bai, J. Zhang and M. Gong, Energy and exergy analysis of heat to salinity gradient power

conversion in reverse electrodialysis heat engine, *Energy Convers. Manag.*, 2022, **252**, 115068.

68 Y. Wang, H. Chen, H. Wang, G. Xu, J. Lei, Q. Huang, T. Liu and Q. Li, A novel carbon dioxide capture system for a cement plant based on waste heat utilization, *Energy Convers. Manag.*, 2022, **257**, 115426.

69 Y. Liu, Y. Chen, J. Ming, L. Chen, C. Shu, T. Qu, Q. Tan, Y. Liu and T. Asefa, Harvesting waste heat energy by promoting H+-ion concentration difference with a fuel cell structure, *Nano Energy*, 2019, **57**, 101–107.

